

2005

Analysis and testing of waste tire fiber modified concrete

Gregory Marvin Garrick

Louisiana State University and Agricultural and Mechanical College, ggarri1@lsu.edu

Follow this and additional works at: https://digitalcommons.lsu.edu/gradschool_theses



Part of the [Mechanical Engineering Commons](#)

Recommended Citation

Garrick, Gregory Marvin, "Analysis and testing of waste tire fiber modified concrete" (2005). *LSU Master's Theses*. 217.
https://digitalcommons.lsu.edu/gradschool_theses/217

This Thesis is brought to you for free and open access by the Graduate School at LSU Digital Commons. It has been accepted for inclusion in LSU Master's Theses by an authorized graduate school editor of LSU Digital Commons. For more information, please contact gradetd@lsu.edu.

**ANALYSIS AND TESTING OF WASTE TIRE
FIBER MODIFIED CONCRETE**

A Thesis

Submitted to the Graduate Faculty of the
Louisiana State University and
Agricultural and Mechanical College
in partial fulfillment of the
requirements for the degree of
Master of Science in Mechanical Engineering

in

The Department of Mechanical Engineering

by
Gregory Marvin Garrick
B.S., Louisiana State University, 2001
May 2005

ACKNOWLEDGEMENTS

I would like to say thanks to God for being with me every step of the way. Next, I would like to say thanks to two of the most wonderful people I have had the pleasure of knowing during my stay at Louisiana State University. I shall simply call them Mr. B and Miss T. Without their support and belief in me, this journey would never have even started. There are not enough words to express my eternal gratitude.

Special thanks to my co-advisors, Dr. Dwayne Jerro and Dr. Guoqiang Li. Many thanks also to Dr. Su-Seng Pang who was a member of my committee I sincerely appreciate all the guidance, advice and support that you have provided in abundance. Thank you all for your contributions.

Many thanks to my loving and wonderful family for their encouragement, and never wavering support. To all my friends, thanks for being with me along the way.

To Randy Young and the staff at the Louisiana Transportation Research Center I would like to say thank you for all their assistance in the preparation and testing of our samples.

The Louisiana Transportation Research Center (LTRC) through a grant to Dr Li and Dr Pang supported this work.

TABLE OF CONTENTS

ACKNOWLEDGEMENTS	ii
LIST OF TABLES.....	v
LIST OF FIGURES.....	vi
ABSTRACT	vii
CHAPTER 1: INTRODUCTION	1
1.1 The Need for Recycling of Waste Tire	1
1.2 Properties of Concrete	3
1.3 Fiber Reinforced Concrete	5
1.3.1 Factors Influencing the Strength and Stiffness of Fiber Reinforced Concrete ..	8
CHAPTER 2: LITERATURE REVIEW	9
2.1 Overview	9
2.2 Experiments Done with Different Rubber Content	9
2.3 Bond Strength between Fiber and Matrix.....	11
2.4 Critical Fiber Length	12
2.5 Finite Element Analysis Background.....	13
2.6 Cracking	14
2.7 Effect of Fiber Orientation and Distribution	15
CHAPTER 3: EXPERIMENTATION.....	16
3.1 Materials and Their Preparation.....	16
3.2 Batch Specifications.....	18
3.3 Testing Procedures	19
CHAPTER 4: ANALYTICAL MODEL	23
4.1 Critical Fiber Length	23
4.2 First Crack Tensile Strength.....	27
4.3 Ultimate Tensile Strength.....	30
CHAPTER 5: FINITE ELEMENT ANALYSIS OF EQUIVALENT FIBER.....	36
5.1 Modeling.....	36
5.2 Meshing.....	37
5.3 Simulation	37
5.4 Solution	38
CHAPTER 6: RESULTS AND DISCUSSION	41
6.1 Compressive and Tensile Strength of Concrete	41
6.2 Modulus of Elasticity	43
6.3 Workability of Concrete	44
6.4 Effect of Waste Tire on Toughness of Concrete	45
6.5 Ductility of Concrete	47
6.6 Waste Tire Chips versus Waste Tire Fibers.....	48

6.7 Analytical and Finite Element Results.....	49
6.8 Uses of Waste Tire Modified Concrete	52
CHAPTER 7: CONCLUSION	53
REFERENCES.....	55
VITA	58

LIST OF TABLES

Table 1: Number of states with regulations on waste tires [http://www.p2pays.org/ref/11/	2
Table 2. The dimensions and distribution of tires and chips in each batch.....	18
Table 3: Efficiency factors, η_1 , for a given fiber orientation relative to the direction of stress.....	48
Table 4. Values used in calculations.....	50

LIST OF FIGURES

Figure 1: Chips used in the experiments.....	19
Figure 2: Fibers used in experiments.....	19
Figure 3: Concrete in compression test.	20
Figure 4: Split tensile strength testing of concrete.	21
Figure 5: Slump testing concrete	21
Figure 6: Comparison of typical slumps [http://www.nrmca.org/ aboutconcrete/cips/CIP%	22
Figure 7: Failure modes of fiber reinforced concrete	28
Figure 8: Constraints and load applied to model.....	38
Figure 9: First cracks formed in concrete surrounding fiber on application of load.	40
Figure 10. Variation of the compressive strength of concrete.....	41
Figure 11: Variation of split tensile strength of concrete.	41
Figure 12: Variation of modulus of elasticity of concrete.....	43
Figure 13: Variation of slump of concrete.	44
Figure 14: Results of air content for concrete.	45
Figure 15: Load displacement results for split tensile testing of rubberized and plain concrete.....	45
Figure 16: Variation of critical fiber length with modulus of elasticity	51

ABSTRACT

There are very serious problems with the disposal of waste tires in the United States. Experiments were conducted to determine how the properties of concrete were affected by the inclusion of waste tires. Waste tires were used in the form of chips and fibers. The fibers were further divided into batches with different lengths to determine the effect of length has on the properties of concrete. There was a noticeable decline in the compressive strength of the concrete; however there was an increase in the toughness of the concrete. It was concluded that waste tire fibers were more suitable as additives than waste tire chips since they produced the highest toughness.

An analytical model was performed to determine how properties such as the critical fiber length affect the ultimate tensile strength of the composite. The ultimate tensile strength of concrete is very important as it is the property that is responsible for the failure of concrete even in compression.

A three-dimensional finite element analysis was performed using ANSYS. Results obtained from this analysis were used to determine the critical fiber length. The models were able to predict a value of ultimate tensile strength that was very close to the experimental result obtained.

CHAPTER 1: INTRODUCTION

1.1 The Need for Recycling of Waste Tire

In 1990, over 240 million scrap tires were discarded in the United States [United States Environmental Protection Agency, 1993] and approximately 3 billion waste tires had accumulated in stockpiles or uncontrolled tire dumps throughout the country, with millions more scattered in ravines, deserts, woods and empty lots [Everett, et al 1998, Jang, et al 1998 and Brown, et al 2001]. Each year, over 77% of the annual production of scrap tires, about 188 million tires per year, were landfilled, stockpiled or illegally dumped [United States Environmental Protection Agency, 1993].

Tires are bulky, and 75% of the space a tire occupies is void, so that the land filling of scrap tires has several difficulties:

- Whole tire landfilling requires a large amount of space.
- Tires tend to float or rise in a landfill and come to the surface.
- The void space provides potential sites for the harboring of rodents.
- Shredding the tire eliminates the above problems but requires high processing costs.

Because of the above difficulties and the resulting high costs, tire stockpiles have turned up across the country. These waste tires represent a significant environmental, human health, and aesthetic problem.

Waste tires pose a health hazard since tire piles are excellent breeding grounds for mosquitoes. Because of the shape and impermeability of tires, they may hold water for long periods providing sites for mosquito larvae development. Waste tires also pose a serious fire hazard since waste tires and waste tire stockpiles are difficult to ignite. However, once ignited tires burn very hot and are very difficult to extinguish. This is due to the 75% void space present in a whole waste tire, which makes it difficult

to quench the tires with water or to eliminate the oxygen supply. In addition, the doughnut-shaped tire casings allow air drafts to stoke the fire. A large tire fire can smolder for several weeks or even months, sometimes with dramatic effect on the surrounding environment. In 1983, a 7-million-tire fire in Virginia burned for almost nine months, polluting nearby water sources [United States Environmental Protection Agency, 1993].

By 1998, 48 states had passed scrap tire laws, regulations or amendments and 34 states provide market incentives to regulate scrap tires. Thirty-five states had banned whole tire landfilling, and eight states had banned any scrap tire landfilling. Only six states did not have any landfill restrictions on tire disposal [http://www.rma.org, 2002]. Sixty percent of scrap tires have been recycled and the stockpiles have decreased to about 500 million tires [http://www.rma.org, 2002]. Even though the situation in the United States has improved, tire stockpiles still exist and pose a threat to public health and safety.

Table 1: Number of states with regulations on waste tires [http://www.p2pays.org/ref/11/10504/html/usa/overview.htm].

	1990 (Number of States)	1996 (Number of States)	1998 (Number of States)
Scrap Tires Legislation/ Regulation	33	48	48
Ban Whole Scrap Tire Landfilling	19*	35	35
Ban Any Scrap Tire Landfilling	1	6	8
Charge Tire Disposal Fee	24	34	30

*Number of states passed landfill restrictions, not ban.

The unique properties of waste tires have made the elimination of waste tire stockpiles difficult. Several of these problems are associated with their toughness (difficult to break down and decompose), durability (difficult to process), shape (large void space, poor space efficiency for storage and transportation) and volume (occupies a large volume).

1.2 Properties of Concrete

Though all Portland cement are basically the same, eight types of cement are manufactured to meet different physical and chemical requirements for specific applications. Type I Portland cement, which is a general Portland cement suitable for most uses was selected for use in this study.

Portland cement is a powdery substance made by burning, at a high temperature, a mixture of clay and limestone producing lumps called “clinkers” which are ground into a fine powder consisting of hydraulic calcium silicates [<http://www.moxie-intl.com/glossary.htm>, 2004].

Portland cement concrete (PCC) is widely used in highway constructions. It has excellent compressive strength but poor tensile strength and very low toughness. This is a phenomenon that is noticed with concrete, that is, if the strength increases then the toughness decreases. It is desired that PCC should have both high toughness and high tensile strength.

The binding quality of Portland cement is due to the chemical reaction between cement and water, called hydration. The less porous the cement paste, the stronger the concrete. In mixing concrete, therefore no more water than is necessary should be used to make the concrete plastic and workable. Advantages of reducing water content:

- Increase compressive and flexural strength
- Increase water tightness

- Lower absorption
- Increase resistance to weathering
- Better bond between successive layers

The hydration reactions by virtue of which Portland cement becomes a bonding agent take place in a water-cement paste. In the presence of water the four major constituents of cement (tricalcium silicate, dicalcium silicate, tricalcium aluminate and tetracalcium aluminoferrite) form products of hydration, which in time produce a firm and hard mass, the hydrated cement paste [Neville, 1996]. The physical properties of the calcium silicate hydrates are of interest in connection with the setting and hardening properties of cement. Hardening in cement refers to the gain of strength of a set cement paste. Mass hardens gradually due to the loss of water either by external drying or by hydration of the inner unhydrated core of the cement grains; in this manner cohesion is obtained.

Attempts have been made to generate strength prediction equations for mortar based on parameters that include, in addition to the main compound composition, terms for SO_3 , CaO, MgO and the water/cement ratio, but the reliability of prediction is marginal.

The strength of concrete depends on the cohesion of the cement paste, on its adhesion to the aggregate particles, and to a certain extent on the strength of the aggregate itself (i.e. its ability to resist the stresses applied to it). There are several forms of strength tests: direct tension, direct compression, and flexure. Flexure determines the tensile strength in bending because hydrated cement paste is considerably stronger in compression than in tension. Strength of concrete is commonly considered its most valuable property. Strength usually gives an overall picture of the quality of concrete because strength is directly related to the structure of the hydrated cement paste. Moreover, the strength of concrete is almost invariably a vital element of

structural design. The shape of the solid particles and their modulus of elasticity also influence the stress distribution and, therefore, stress concentration, within concrete.

1.3 Fiber Reinforced Concrete

A major reason for the growing interest in the performance of fibers in cement-based materials is the desire to increase the toughness or tensile properties of the basic matrix. Fiber reinforced concrete was created to combine the tensile strength of rubber with the compressive strength of concrete. It was also intended to increase the toughness of concrete by including waste tires as fibers into the matrix. Waste tires possess high toughness and this property is hoped to be imparted to the concrete. This is an example of a fiber-reinforced composite.

Composites consist of one or more discontinuous phases embedded in a continuous phase. The discontinuous phase is usually harder and stronger than the continuous phase and is called the reinforcement or reinforcing material, whereas the continuous phase is called the matrix [United States Environmental Protection Agency, 1993].

The resultant properties of composites are strongly influenced by the properties of their constituent materials, their distribution, and the interaction among them. The composite properties may be the volume fraction sum of the properties of the constituents, or the constituents may react in a synergistic way so as to provide properties in the composite that are not accounted for by a simple volume-fraction sum of the properties of the constituents. Thus in describing a composite material as a system, besides specifying the constituent materials and their properties, we need to specify the geometry of the reinforcement with reference to the system. The geometry of the reinforcement may be described by the shape, size, and size distribution.

The size and size-distribution control the texture of the material. Together with volume fraction, they also determine the interfacial area, which plays an important role in determining the extent of the interaction between the reinforcement and the matrix.

Fiber reinforced concrete is being developed to improve the mechanical properties such as stiffness and toughness. The strengthening mechanism depends on the geometry of the reinforcement. As a result, composite materials are classified based on the geometry of a representative unit of reinforcement. Chips and fibers were used in conducting the research. A chip is characterized by its width being almost equal to its length while a fiber is characterized by its length being much greater compared to its cross-sectional dimensions. The greater part of this thesis was devoted to fibers since they were found to be more desirable as additives to the concrete matrix.

The dimensions of the reinforcement determine its capability of contributing its properties to the composite. In addition, a reinforcement having a long dimension discourages the growth of incipient cracks normal to the reinforcement that might otherwise lead to failure, particularly with brittle matrices. Therefore, fibers are very effective in improving the fracture resistance of the matrix. The composite may fail in a single-fracture mode or, if the fiber volume content is high, it is possible to reach the multiple-cracking stage of the matrix.

Fibers were embedded in matrix material (concrete) to form a fibrous composite. The matrix performs several tasks, including binding the fibers together and transferring loads to the fibers. Reinforcements may be short or long compared to their overall dimensions. Composites with short fibers are called discontinuous-fiber-reinforced composites while those with long fibers are called continuous fiber-reinforced concrete. The fiber length affects the properties of discontinuous-fiber-reinforced composite. The load-transfer mechanism of the matrix is more important in discontinuous-fiber-reinforced composite than in continuous fiber composites. In a discontinuous-fiber

composite, the fiber length affects the properties of the composite. This was investigated in this thesis. The orientation of the waste tire fibers cannot be easily controlled in the composite. The fibers are randomly distributed in the matrix

One of the most important factors determining the properties of composites is the relative proportion of the matrix and reinforcing materials. The relative proportions can be given as the volume fraction. Volume fractions are used in the theoretical analysis of composite materials. If the volume (v_c) of a composite material that consists of volume (v_f) of the fibers and volume (v_m) of the matrix material, then the volume fraction can be denoted by V . Therefore, the volume fractions are defined as follows:

$$V_f = \frac{v_f}{v_c}, \quad V_m = \frac{v_m}{v_c}$$

where $v_c = v_f + v_m$.

V_f = Volume fraction of fiber

V_m = Volume fraction of matrix

In composites, loads are not directly applied on the fibers but are applied to the matrix material and transferred to the fibers through the fiber ends and also through the cylindrical surface of the fiber near the ends. In the case of short-fiber composites, the end effects cannot be neglected and the composite properties are a function of the fiber length.

Experiments were conducted using both chips and fibers in the concrete. The fibers used were of various lengths and aspect ratios. A finite element analysis was conducted on a representative section of the composite sample. Results from these simulations were used in a numerical model that was created. A numerical analysis was conducted to determine a few of the most important properties of the fibers that

directly affect the characteristics of the composite, such as the critical fiber length and the ultimate tensile strength of the composite. Cox's shear lag theory was used to create the model [Cox, 1952]. The critical fiber length is a very important parameter as this has direct implications on the ultimate tensile strength of the samples, which controls the cracking phenomenon.

1.3.1 Factors Influencing the Strength and Stiffness of Fiber Reinforced Concrete

Factors influencing the strength and stiffness of fiber reinforced concrete are [Agarwal, 1980]:

1. Misorientation of fibers
2. Fibers of non-uniform strength
3. Discontinuous fibers
4. Interfacial conditions
5. Residual stress

Agarwal found that fiber orientation directly affects the distribution of loads between the fibers and the matrix. He deduced that there was maximum contribution to the composite properties from the fibers only when they are parallel to the loading direction. The strength and stiffness of the composite will be reduced when the fibers are not parallel to the loading direction. The extent to which the strength and stiffness may be reduced depends on the angle to the loading axis or the number of fibers that are not parallel to the loading direction.

If there is a reduction in fiber strength there will be a resultant reduction in composite strength. As a result, if all the fibers are uniform in their strength values a high strength composite will be obtained. In the concrete, load is not directly applied to the fibers, but to the matrix material and is transferred to the fibers through the fiber ends.

CHAPTER 2: LITERATURE REVIEW

2.1 Overview

Concrete is one of the two most commonly used structural materials [Neville, 1996]. During the 1970's with the onset of the energy crisis and along with the increase in environmental consciousness a lot of focus was placed on the use of industrial waste products such as waste tire as an additive to concrete [Topcu, 1995]. Topcu in his study investigated the changes of the properties of rubberized concretes in terms of both size and amount of the rubber chips. The compressive strength when tested at 28 days was 29.50MPa, it was however shown that that with the addition of 15, 30 and 45% of coarse rubber chip, that value was reduced to 14.60, 8.91 and 5.51 MPa respectively. This represents a 51, 70 and 81 percent reduction in compressive strength.

It was considered that the rubberized concrete would be very suitable to be used in jersey barriers in which high strength is not necessary, however toughness is desired as it is subjected to direct impact in crashes. The rubberized concrete could reduce the damage to vehicles and also reduce the loss of lives from accidents.

The disposal of waste tires represents a major issue in the solid waste dilemma because there are more than 242,000,000 scrap tires, approximately one tire per person, generated each year in the United States (Epps, 1994). Therefore, over the past few years, a number of researches have been focused on the use of waste tires in different shapes and sizes in concrete.

2.2 Experiments Done with Different Rubber Content

Experiments were conducted [Eldin, et al., 1993] to examine the strength and toughness properties of rubberized concrete mixtures. They used two types of tire rubber with different rubber content. Their results indicate that there is about an 85% reduction in compressive strength, whereas the tensile strength reduced to about 50%

when the coarse aggregate was fully replaced by rubber. A smaller reduction in compressive strength (65%) was observed when sand was fully replaced by fine crumb rubber. Concrete containing rubber did not exhibit brittle failure under compression or split tension. A more in-depth analysis of their results indicates a good potential of using recycled rubber in Portland cement concrete mixtures because it increases fracture toughness. However, an optimized mix design is needed to optimize the tire rubber content in the mixture.

Recycled waste tire rubber was also investigated as an additive to Portland cement concrete [Zaher, et al, 1999]. Two types of waste tire rubber were used, fine crumb rubber and coarse tire chips. The study was divided into three groups. In the first group only crumb rubber was used and only replaced the fine aggregates. In the second group tire chips were used to replace the coarse aggregates. In the third and final group both crumb and chips were used. In this group the rubber content was equally divided between crumb and chips, and again the crumb replaced fine aggregates while the chips replaced the coarse aggregates. The rubber content used in the three groups ranged from 5-100%. The aggregates were partially replaced by the rubber. They found that rubberized PCC can be made and are workable (even though greatly reduced) with the rubber content being as much as 57% of the total aggregate volume. Their results showed that the reduction in strength was too great, thus they recommended not replacing more than 20% by volume of the aggregate with waste tires.

Researchers have tried to gain different advantages from the use of waste tire in concrete. High-strength concrete (HSC) with silica fume was modified with different amounts of crumbed truck tires [Hernandez-Oliveres, et al 2003]. They were aiming to reduce the stiffness of HSC to make it compatible with other materials and building elements, unexpected displacement of building foundations and improving the fire performance of the buildings.

They found that since water vapor can escape through the channels left as the waste tire particles are burned, the inclusion of low volume fractions of rubber would reduce the risk of explosive spalling of HSC at high temperature. This was very desirable since HSC was more susceptible to explosive spalling when subjected to rapid heating than normal strength concrete.

Samples containing 0%, 3%, 5% and 8% waste tires were made. Mechanical, destructive and non-destructive tests were performed on the samples and it was found that volume fractions up to 3% do not significantly reduce the strength of the composite although it does reduce the stiffness. Higher volumes of rubber result in a reduction of strength but improve the dynamic behavior of the concrete.

2.3 Bond Strength between Fiber and Matrix

The main factors controlling the theoretical performance of the composite material are the physical properties of the fibers and the matrix, and the strength of the bond between the two. Bond strengths vary with a wide variety of parameters, including time.

From several experiments conducted, one of the general conclusions was that there was a reduction in compressive, flexural and tensile strength. Several authors have suggested that the loss in strength might be minimized by prior surface treatment of the waste tire [Lee, et al. 1993 and Raghavan, et al. 1998]. The bonding between concrete matrix and waste tire is not very strong. A study was conducted [Segre, et al. 2000] in which the surface of powdered rubber tire was modified with several surface treatments including sodium hydroxide (NaOH), to increase the hydrophilicity of the rubber surface. It was assumed that by doing this, the sodium hydroxide would hydrolyze the acidic and/or carboxyl groups present on the rubber surface [Smith, et al, 1995]. The samples were cured for 28 days then tested.

To determine the nature of the bond between the rubber-cement matrix interfaces, micrographs of the samples were obtained by using a scanning electron microscope (S.E.M.). Micrographs of the fracture surface of a cement sample with 10% rubber showed a bulk region and the rubber particles seem to have been pulled-out. It was also noted that there was less pull out from the matrix for the NaOH treated rubber than for the untreated rubber. Discontinuity was seen in the rubber-matrix interface implying that the rubber adhesion to cement paste is poor. When the same analysis was done on the waste tire treated with NaOH, an adhesive joint was observed between the rubber and the matrix. Electron microscopic examinations showed that the sodium hydroxide surface treatment improved the waste tire – matrix adhesion.

Flexural strength, modulus of elasticity, compressive strength and abrasion resistance test were done using samples containing 10% of sodium hydroxide treated rubber. They found that for flexural strength the specimen with NaOH-treated rubber showed higher values than the control specimen.

2.4 Critical Fiber Length

A very important property of the reinforcements is their critical fiber length. When fibers are smaller than the critical length, the maximum fiber stress is less than the average fiber strength so that the fibers will not fracture, regardless of the magnitude of the applied stress [Agarwal, et al. 1980]. The composite failure occurs when the matrix or interface fails. In the case of discontinuous-fiber reinforced concrete, an additional factor influences the failure, namely, the large stress concentrations in the matrix produced as a result of the fiber ends. The result of the stress concentration is to further lower the composite strength [Agarwal, et al. 1980].

2.5 Finite Element Analysis Background

The main obstacle to finite element analysis of reinforced concrete structures is the difficulty in characterizing the material properties. Much effort has been spent in search of a realistic model to predict the behavior of reinforced concrete structures. Due mainly to the complexity of the composite nature of the material, proper modeling of such structures is a challenging task. Despite the great advances achieved in the fields of plasticity, damage theory and fracture mechanics, among others; a unique and complete constitutive model for reinforced concrete is still lacking [Barbosa, et al. 1998].

Software developers implement the nonlinear material laws into finite element analysis codes in one of two ways [Fanning, 2001]. One method is to program the material behavior independently of the elements to which it may be specified. In this method, the choice of element for a particular physical system is not limited. This is the most versatile approach and does not limit the analyst to specific element types in configuring the problem of interest. The other method is to have specific specialized nonlinear material capabilities only with dedicated element types. The latter method is found in ANSYS. For concrete, it has a dedicated three-dimensional eight node solid element, SOLID65, to model the nonlinear response of brittle materials based on the constitutive model for the triaxial behavior of concrete proposed by Willam and Warnke [Willam, et al. 1975]. The element type used for rubber was SOLID185 which was defined by orthotropic material properties and eight nodes having three degrees of freedom at each node: translations in the nodal x, y, and z directions. The element has plasticity, hyperelasticity, stress stiffening, creep, large deflection, and large strain capabilities.

2.6 Cracking

When a microcrack is produced in the matrix several alternate effects may take place [Hannant, 1978]. He found that if the microcrack is close to the fiber the interface shear stresses would separate the fiber from the remaining composite by propagating the crack along the length of the fiber. Alternatively, the crack may propagate out in a direction normal to the fibers across the other fibers, because of the local stress concentrations, leading to immediate composite fracture. Each crack that is formed causes stress redistribution in its vicinity.

The composite is affected by the interfacial condition because the interfacial bond between the matrix and the fibers is an important factor influencing the mechanical properties and performance of composites. The interface is responsible for transmitting the load from the matrix to the fibers, which contribute to the greater portion of the composite strength. The mechanism of load transfer through the interface becomes more important in the discontinuous-fiber-reinforced composites [Hannant, 1978]. When a strong bond exists between the fibers and the matrix, the cracks still do not propagate along the length of the fibers. A strong bond is also important for the higher transverse strengths.

In concrete, internal material failure generally initiates before any change in its macroscopic appearance or behavior is observed. Internal material failure may be in several forms including microcracking of the matrix and separation of the fibers from the matrix.

As the load is increased after the modulus of rupture is exceeded, cracks begin to develop. When concrete cracks, a sudden drop of tensile strength across the cracks occurs. This creates a non-equilibrium state in the concrete structure. The residual stress from the non-equilibrium state is redistributed to another part of the structure.

In the single-fracture mode the bridging of fibers across the crack to transfer the load is usually simulated by pullout tests. However, in the multiple-cracking mode the simulation is no longer possible, because the force distribution in the fiber between the cracks is no longer similar to that in the pull-out test [Kullaa, 1994].

2.7 Effect of Fiber Orientation and Distribution

Researchers have found several benefits of waste tire fiber concrete on the effect of fibers on the resistance of the concrete to cracking:

1. Increases in the load at which visible cracks are formed under flexural loading [Snyder, et al. 1972].
2. Resistance to cracking under impact loading [Hoff, 1975].
3. Prevention of cracking in slabs subjected to shrinkage conditions [Elvery, et al. 1975] or limitation of cracking in highway pavements that contains fibers [Johnston, 1975].

Cracking generally applies to cracks greater than about 0.05 mm, i.e. just visible to the naked eye and waste tire fibers can delay the appearance of cracking at this level. The fibers have little effect on the crack initiation point at the microscopic level [Edginton, et al. 1974].

The arrangement of the fibers in the matrix has an important influence on their strengthening and toughening capability. A fiber oriented parallel to the direction of the applied stress or perpendicular to a propagating crack has maximum effect, while one perpendicular to the stress or parallel to the crack has no effect. Also, concentrating fibers in regions of maximum stress makes more efficient use of a given amount of fibers. In the concrete mass the fiber orientation is 3-dimensional random, and strengthening and toughening occur uniformly in all directions.

CHAPTER 3: EXPERIMENTATION

3.1 Materials and Their Preparation

Concrete strength is greatly affected by the properties of its constituents and the mixture design parameters. In performance of the experiments the raw materials used included Portland cement, Davanair 1000, mixture of aggregates (coarse and medium), sand, water and tire fibers. Tires from light vehicles, such as cars and from heavy vehicles such as trucks were used. The tires were cut by hand and a band saw obtained from the Engineering Workshop at Louisiana State University. Tires from light vehicles had smaller and fewer wires than those from heavy vehicles. They were cut into strips of 25.4mm (1in) x 5mm (0.2in) x 5 mm (0.2in), 50.8 mm (2in) x 5mm (0.2in) x 5mm (0.2in) and 76.2 mm (3in) x 5mm (0.2in) x 5 mm (0.2in).

Daravair® 1000 is a liquid air-entraining admixture that provides freeze-thaw resistance, yield control, and finishability performance across the full range of concrete mix designs. Air-entrained concrete is one in which minute air bubbles are intentionally trapped by the addition of an admixture to the cement during the batching and mixing of the concrete. The presence of a properly distributed amount of these bubbles imparts desirable properties to both freshly mixed and hardened concrete. In freshly mixed concrete, entrained air acts as a lubricant, improving the workability of the mix, thereby reducing the amount of water that needs to be added.

In the experiments, fifteen percent by volume of fibers was used. This value was chosen for the fact that from experiments that have been conducted [Khatib, et al. 1999] it was found that if greater than 20 percent was used the strength and toughness of the concrete would be so low that the material would not be usable. On the other hand, if less than ten percent was used it would not be economically viable.

In introducing the fibers into the mix, it was ensured that there was single fiber addition and the fibers reached the mixer individually and were immediately removed from the point of entry by the mixing action, so as to produce uniform fiber distribution.

The concrete mixed used was rated at 40MPa compression strength. A control PCC mix was designed using American Concrete Institute Standard 211.1 mix design methods for the modified batches to be compared with. In the modified batches, fifteen percent of the coarse aggregates were replaced by tires as mentioned previously. The mix ratio by weight for control concrete was cement: water: gravel: sand: DARAVAIR 1000 = 1: 0.50: 3.50: 1.88: 0.001. The mix ratio by weight for rubberized concrete was cement: water: gravel: waste tire: sand: DARAVAIR 1000 = 1: 0.50: 3.40: 0.10: 1.88: 0.001.

Two different size samples were made. The dimensions of the samples were 6-inch diameter by 12-inch length and 4-inch diameter by 8-inch length. They were cured for 28 days in a controlled environment at the Louisiana Transportation Research Center. This time was chosen since concrete hardens and gain strength as it hydrates. The hydration process continues over a long period of time. It happens rapidly at first and slows down as time goes by. To measure the ultimate strength of concrete would require a wait of several years. This would be impractical, so a period of 28 days was selected by specification writing authorities as the age that all concrete should be tested. At this age, a substantial percentage of the hydration has taken place [http://www.cement.org/basics/concretebasics_faqs.asp, 2003].

After the concrete was mixed, it was placed in a container to set. A satisfactory moisture content and temperature (between 50°F and 75°F) must be maintained, a process called curing. Adequate curing is vital to quality concrete. Curing has a strong influence on the properties of hardened concrete such as durability, strength, water tightness, abrasion resistance and volume stability. Surface strength development can

be reduced significantly when curing is defective. Curing the concrete aids hydration; most freshly mixed concrete contains considerably more water than is required for complete hydration of the cement; however, any appreciable loss of water by evaporation or otherwise will delay or prevent hydration. If temperatures are favorable, hydration is relatively rapid the first few days after concrete is placed; retaining water during this period is important. Good curing means evaporation should be prevented or reduced.

3.2 Batch Specifications

Seven batches of six-inch radius by twelve-inch height cylinders were prepared. One batch was made without waste tires to be the control while six batches were prepared using waste tire chips or fibers. Thirty were prepared using fibers of lengths one inches, two inches and three inches while one batch was made using chips. Chips used were from light duty vehicle (cars) and heavy duty vehicles (trucks) approximately in a one to one ratio. Steel belts were included in some of these tires. The details of the composition are given in Table 2.

Table 2. The dimensions and distribution of tires and chips in each batch.

Batch number	Waste tire shape	Fiber/chip length (in)	Fiber/chip width (in)	Fiber/chip height (in)
1	N/A	N/A	N/A	N/A
2	Truck and car rubber chips with steel wires	1	1	0.2
3	Car tires without steel wires	1	0.2	0.2
4		2	0.2	0.2
5		3	0.2	0.2
6	Car tires with steel wires	2	0.2	0.2
7	Truck and car tire with steel wires	2	0.2	0.2

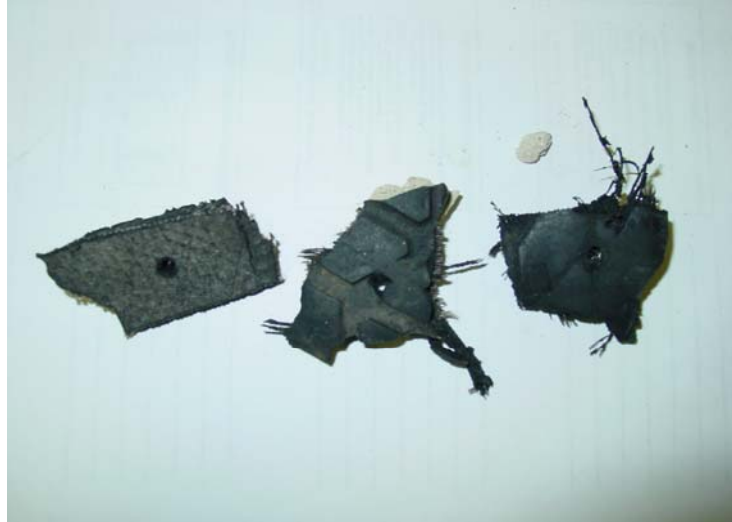


Figure 1: Chips used in the experiments.



Figure 2: Fibers used in experiments

The fibers were from car tires only or a mixture of car and truck tires in a one to one ratio. Different fiber lengths were used to determine the effect of fiber aspect ratio on the properties of concrete such as stiffness and strength.

3.3 Testing Procedures

There are a series of standardized testing procedures for determining concrete material properties. The response of a reinforced concrete structural element is determined in part by the response of plain concrete in compression. As a result,

standard practice in the United States [ACI, 1992] recommends characterizing the response of concrete on the basis of the compressive strength of a 6 inch diameter by 12 inch long (152.4 mm by 304.8 mm) concrete cylinder. For typical concrete mixes, the standard cylinder is sufficiently large that the material is essentially homogeneous over the critical zone. Additionally, while the standard procedure (ASTM C39) does not require efforts to reduce frictional confinement induced during testing at the ends of the specimen, the specimen is considered to be sufficiently long that approximately the middle third of the cylinder experiences pure compression.

After being cured, the samples were then subjected to split tensile strength, compressive strength and compressive modulus tests. An MTS machine was used to perform these tests.



Figure 3: Concrete in compression test.



Figure 4: Split tensile strength testing of concrete.

Samples from each of the batches were tested. ASTM C 39 Standard was used in conducting compressive tests (Figure 3) while ASTM C496-86 Standard was used for the split tensile strength tests (Figure 4).



Figure 5: Slump testing concrete

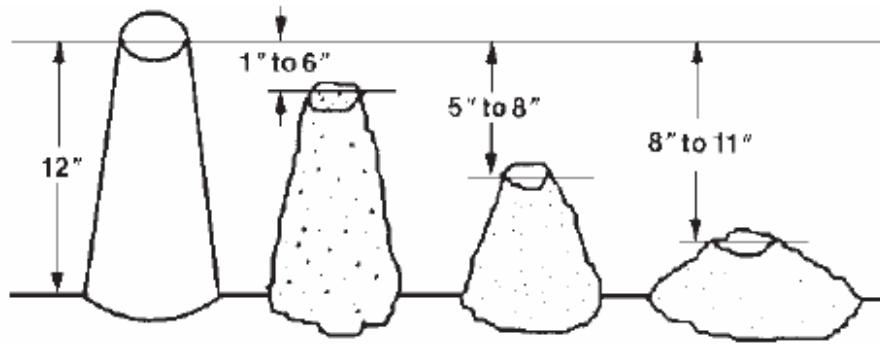


Figure 6: Comparison of typical slumps [<http://www.nrmca.org/aboutconcrete/cips/CIP%2022p.pdf>].

Slump tests were also conducted to measure the workability or consistency of concrete. Workability is the relative ease or difficulty of placing and consolidating concrete. When placed, all concrete should be as stiff as possible, yet maintain a homogeneous, voidless mass. Too much stiffness, however, makes it too difficult or impossible to work the concrete into the forms and around reinforcing steel. On the other hand, too fluid a mixture is also detrimental. The measure of the workability or consistency of concrete is its slump, which is a design consideration that is inversely proportional to the stiffness of the mix. The slump should never exceed six inches (15.24 cm). Slump test was performed according to ASTM C 143 Figure 5. A comparison of different slumps is shown in Figure 6.

CHAPTER 4: ANALYTICAL MODEL

There are several parameters that affect the performance of concrete. Two of the most important parameters are the ultimate tensile strength and the critical fiber length. Analytical models will be developed to predict both these properties. By knowing how these parameters affect the performance of waste tire modified concrete then the design can be optimized to produce a better composite.

In developing these models, assumptions were made that the fibers were uniformly distributed in the concrete matrix and were of uniform strength. The tensile strength is extremely important because it is considered to be the factor that is responsible for the failure of the concrete, even in compression. This is so since when concrete is uniaxially tested by compression, Poisson's effect causes tensile stresses to be developed perpendicular to the application of load. Since the tensile strength of concrete is approximately one tenth of its compressive strength the sample will fail due to tension before the sample is crushed as a result of compression.

Knowing the above properties and knowing how they vary and what affects them, then suitable modifications can be made to produce a superior composite.

Due to the introduction of coarse aggregates in the concrete, the distribution of fibers in the space will be disturbed by the coarse aggregates. The space already occupied by the coarse aggregates cannot be occupied by the fibers again. The fibers can distribute only in the remaining space. This space is called the effective space. The effective space is determined based on the mixture ratio of every component in concrete and the aggregate gradation.

4.1 Critical Fiber Length

The reinforcing efficiency of fibers is closely related to fiber length. For discrete fiber reinforced concrete, a critical fiber length, l_c , is defined as the minimum fiber length

required for the build-up of a stress (or load) in the fiber which is equal to its strength (or failure load). If fiber length is smaller than l_c , there is no sufficient embedded length to generate a stress equal to the fiber strength, and the fiber is not used efficiently. Only if the length of fibers considerably exceeds l_c does the stress along most of the fibers reach its yield or tensile strength, thus mobilizing most of the potential of the fiber reinforcement.

Critical fiber length is the maximum value of load-transfer length. It is an important system property and affects ultimate composite properties. Over this length the fiber supports a stress less than the maximum fiber stress.

There is a critical length, l_c , which the fibers must have to strengthen a material to their maximum potential. Critical fiber length is twice the length of fiber embedment that would cause fiber failure in a pull out test [Hannant, 1978]. This critical length is given by equation (1) below. According to Kelly [Kelly, et al. 1971]

$$l_c = \frac{\sigma_f r}{\tau_s} \quad (1)$$

where σ_f = Ultimate strength of fiber

τ_s = Frictional shear strength at fiber-matrix interface

r = Radius of fiber used. For square fibers $r = a/\sqrt{\pi}$, where a is the length of the side of the square cross-section.

Cox shear lag theory [Cox, 1952] was used to obtain l_c .

Assumptions:

1. Fiber surrounded by cylindrical matrix

2. Transfer of load from matrix to fiber depends on the difference between the actual displacement at a point on the interface, at a distance x from the end of the fiber, and displacement that would be observed if the fiber was absent.
3. A perfect bond exists between fiber and matrix.
4. No load transfer through ends of fiber.

Cox's result for tensile stress in fiber (σ) and shear stress along fiber/matrix interface (τ) for a fiber with length l was:

$$\sigma(x) = \frac{E_f}{E_m} \sigma_m \left[1 - \frac{\cosh \beta(l/2 - x)}{\cosh \beta l/2} \right] \quad (2)$$

$$\tau(x) = \frac{\beta E_f}{2 E_m} \sigma_m \frac{\sinh \beta(l/2 - x)}{\cosh \beta l/2} \quad (3)$$

Where x = distance from end of fiber

σ_m = stress in matrix

$$\beta = \frac{1}{r} \left[\frac{E_m}{(1 - \nu_m)(E_f - E_m) \ln(R/r)} \right]^{0.5} \quad (4)$$

Where R = Half distance between neighboring fibers

ν_m = Poisson's ratio of the matrix

r = Radius of fiber

To make full use of the load carrying capacity of the fibers, the failure criterion can be determined as the fiber breaking and interfacial debonding. It is known that the maximum fiber axial stress is at the middle of the fiber ($x = l/2$), the maximum interfacial shear stress is at the ends of the fiber ($x = 0$ or $x = l$). Let $l = l_c$, substitute $x = l_c/2$ and $\sigma(x) = \sigma_f$ into Equation (2), $x = 0$ and $\tau(x) = \tau_s$ (matrix shear strength) into Equation 3. Divide Equation 2 by 3, gives the critical fiber length as

$$l_c = 2r \left(\frac{E_m}{E_f} \right)^{0.5} \sqrt{\ln(R/r)(1 + \nu_m)} \left[\ln \frac{1 + k \sigma_f / \tau_s}{1 - k \sigma_f / \tau_s} \right] \quad (5)$$

$$\text{where } k = \sqrt{\frac{G_m}{2E_f \ln(R/r)}}$$

This represents the critical fiber length expression for fibers uniformly distributed in the matrix. In concrete, the aggregate will disturb the fiber distributions in the matrix. The space already occupied by the aggregates cannot be occupied by the fibers. Therefore, the fibers cannot display its reinforcing effect in the space occupied by the coarse aggregate. The fibers can become bridging fibers only in the remaining space. The aggregate will disturb the fiber distributions in the matrix of the concrete. For aggregates with smaller size, such as sand, the disturbances can be neglected. The space already occupied by the aggregates cannot be occupied by the fibers.

The volume fraction of the effective space in the critical zone can be estimated as

$$f_e = 1 - [1 - P(d_a)] f_a \quad (6)$$

where f_e = volume fraction of effective space

f_a = volume fraction of aggregate

$P(d_a)$ = percent passing of graded aggregates

$$P(d_a) = \left(\frac{d_a}{d_{a_{\max}}} \right)^m \quad (7)$$

$$R = r \sqrt{\frac{f_e}{f_{fc}}} \quad (8)$$

where R = half-distance between neighboring fibers

f_{fc} = volume fraction of fibers in concrete

Substitute 6-8 into 5

$$l_c = 2r \left(\frac{E_m}{E_f} \right)^{0.5} \sqrt{0.5 \ln(f/f_{fc}) (1 + \nu_m)} \ln \left[\frac{1 + k_o \sigma_f / \tau_s}{1 - k_o \sigma_f / \tau_s} \right] \quad (9)$$

In which $k_o = \sqrt{\frac{G_m}{E_f \ln(f/f_{fc})}}$

4.2 First Crack Tensile Strength

Preliminary modeling of the first crack tensile strength was done. Discontinuous short fiber reinforced concrete has four types of failure modes, depending on the fiber volume fraction, fiber aspect ratio and interfacial bonding strength as shown in Figure 7. In Figure 7(a) and (b), the composite fail catastrophically, even though the first crack strength and the fracture toughness of the composite would still be higher than that of the concrete matrix. This is as a result of the low fiber volume fraction, small fiber aspect ratio, and large initial defect. These failure modes show a lack of reinforcing effect thus they are not suitable for as structural materials.

The failure modes shown in Figure 7(c) and (d) occur when an adequate fiber volume fraction, high fiber aspect ratio and small initial defect are combined. In Figure 7(c), the first crack strength, σ_o , is follow by a sudden drop in load bearing capacity, with a subsequent rise to σ_u , the ultimate strength of the composite, before final softening as a single crack enlarges. As a result of the sudden drop of strength following the first crack, this is not considered an optimal failure mode for structural applications. Figure 7 (d) show an ideal failure mode for both strengthening purpose and repairing purpose. This can be achieved if the initial defect in the composite is further reduced.

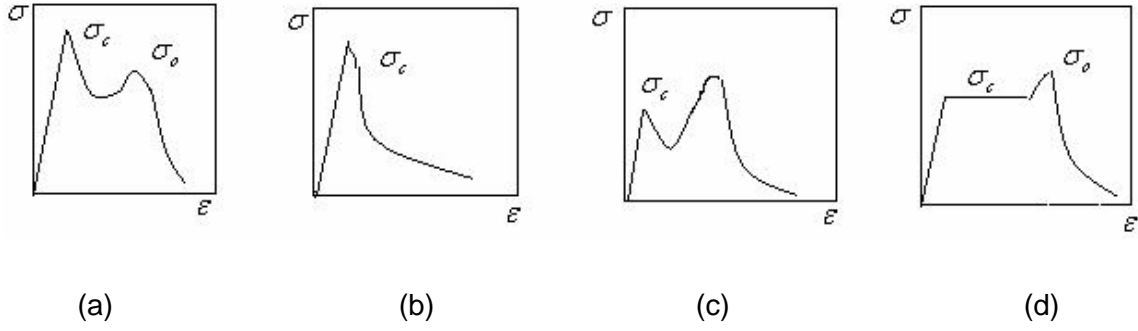


Figure 7: Failure modes of fiber reinforced concrete

The following assumptions are made in estimating the first crack strength of fiber reinforced concrete:

- In each sample all fibers have the same length and the same diameter.
- All fibers have the same strength.
- The fibers are uniformly distributed in the effective space.
- Interfacial bond is perfect before the fiber breaking/interfacial debonding criterion is reached.

The effective space was given in Equation 6. Using the rule-of-mixtures method, the first crack strength of fiber reinforced concrete can be expressed as

$$\sigma_c = \eta_l \eta_\theta E_f \varepsilon_{um} f_f + \sigma_{um} (f_e - f_f) + \sigma_i (1 - f_e)(1 - k_1) + \sigma_{ci} (1 - f_e) k_1 \quad (10)$$

Where σ_c = first crack strength of waste tire reinforced concrete

η_l = fiber reinforcing efficiency factor related to the fiber length

η_θ = fiber reinforcing efficiency factor related to the fiber orientation

ε_{um} = ultimate tensile strain concrete with aggregate diameter smaller than 5 mm.

σ_{um} = ultimate strength of concrete with aggregate diameter smaller than 5 mm.

σ_i = ultimate tensile strength for un-clustered aggregates with aggregate diameter greater than 5 mm.

σ_{ci} = ultimate tensile strength for concrete consisting of clustered aggregates

with aggregate diameter greater than 5 mm.

$k_1 =$ is the corresponding aggregate cluster ratio.

The cluster ratio of coarser aggregates over the first crack plane is dependent on the maximum aggregate size, aggregate gradation, and the mixing effort. For a perfect mixing, the aggregate will be uniformly distributed in the space. This will make $k_1 = 0$.

If fiber intercepts or bridges over the first crack plane when the first crack occurs, the fiber will contribute to the strength of the reinforced concrete. If the fiber does not bridge the crack, it will have no contribution to the first crack strength of the reinforced concrete. Thus the fiber length efficiency factor can be determined through the probability of a fiber intercepting or bridging over the first crack plane. Applying the theory of statistics, the fiber length efficiency factor, η_l , is obtained as follow

Fiber length efficiency factor, η_l [Allen, 1975]

$$\begin{aligned} \eta_l &= 1 - l_c/2l & (l > l_c) \\ \eta_l &= l/2l_c & (l < l_c) \end{aligned} \tag{11}$$

The probability density function of the distribution of the fiber orientation in a three dimensional space is

$$p(\theta) = \frac{1}{A} \frac{dA}{d\theta} = \frac{2\pi l^2 \sin \theta}{2\pi l^2 (\cos \theta_1 - \cos \theta_2)} = \frac{\sin \theta}{(\cos \theta_1 - \cos \theta_2)} \tag{12}$$

Where l_e is the fiber embedded length in the matrix and θ is the fiber orientation angle, $\theta_1 < \theta < \theta_2$. If the fiber is freely distributed in the three-dimensional space, then $\theta_1 = 0$ and $\theta_2 = \pi/2$.

If we consider an inclined fiber with angle θ , the embedded length of a fiber in the tension direction has a factor $\cos \theta$, then the fiber orientation reinforcing efficiency factor can be solved as shown below for a three dimensional structure

$$\eta_{\theta} = \int_{\theta_1}^{\theta_2} p(\theta) \cos \theta d\theta = \frac{\sin^2 \theta_2 - \sin^2 \theta_1}{2(\cos \theta_1 - \cos \theta_2)} \quad (13)$$

Substitute 11-13 into 10, the first crack strength of reinforced concrete can be obtained as follow

$$\sigma_c = \frac{(\sin^2 \theta_2 - \sin^2 \theta_1)}{2(\cos \theta_1 - \cos \theta_2)} \left(1 - \frac{l_c}{2l_c}\right) E_f \varepsilon_{um} f_f + \sigma_{um} (f_e - f_f) + \sigma_i (1 - f_e)(1 - k_1) + \sigma_{ci} (1 - f_e) k_1$$

$$(l > l_c) \quad (14)$$

$$\sigma_c = \frac{(\sin^2 \theta_2 - \sin^2 \theta_1)}{2(\cos \theta_1 - \cos \theta_2)} \frac{l}{l_c} E_f \varepsilon_{um} f_f + \sigma_{um} (f_e - f_f) + \sigma_i (1 - f_e)(1 - k_1) + \sigma_{ci} (1 - f_e) k_1$$

$$(l < l_c)$$

4.3 Ultimate Tensile Strength

In determining the ultimate tensile strength (UTS), the same assumptions were made as for the first crack strength. After the first crack and the multiple crack process, the ultimate cracking of the concrete may occur if loads are continuously applied. Since the concrete matrix has cracked before the ultimate strength is reached, the applied loads will be carried only by the reinforcing fibers. The ultimate strength can be expressed as

$$\sigma_o = cf(\sigma_{bf}, \sigma_{ubf}) \quad (15)$$

where σ_o = UTS of short fiber reinforced concrete

c = Factor accounting for distribution of fibers in space

$f(\sigma_{bf}, \sigma_{ubf})$ = Strength contribution of fibers as shown below $f(\sigma_{bf}, \sigma_{ubf})$

$$f(\sigma_{bf}, \sigma_{ubf}) = \sigma_{bf} + \sigma_{ubf} \quad (16)$$

σ_{bf} & σ_{ubf} = Strength contribution of bridging fiber and unbridging fibers, respectively.

Using the theory of statistics and the geometry principle, the factors $f(\sigma_{bf}, \sigma_{ubf})$ and c can be obtained as shown below. The number of fibers in a unit area, N_a , and in an unit volume, N_v , has the following relation

$$N_a = \frac{l}{2} N_v \quad (17)$$

For uniform distribution of fibers in the effective space, the number of fibers per unit volume is

$$N_v = \frac{\varphi_f}{\pi r_f^2 l} \quad (18)$$

Substituting Equation 18 into Equation 17 gives

$$N_a = \frac{\varphi_f}{2\pi r_f^2} \quad (19)$$

When a large number of fibers distribute unidirectionally, the probability for bridging fibers is

$$P_b = \begin{cases} 1 - l_c/l < 1 & (l_c/l < 1) \\ 0 & (l_c/l > 1) \end{cases} \quad (20)$$

P_b is the ratio of bridging fibers to the total fibers at the cross-section.

For the fibers distributed in three dimension, the average projecting length of fibers, l_a , in the tension direction is

$$l_a = l/2 \quad (21)$$

Thus the average angle of fibers in space is

$$\theta_a = \cos^{-1}(l_a/l) = \pi/3 \quad (22)$$

For a fiber with an angle θ , its projecting length in the tension direction is

$$l' = l \cos \theta \quad (23)$$

Among all the fibers, the average length for bridging fibers in the tension direction is

$$l'_{ba} = \frac{1}{\theta_c} \int_0^{\theta_c} l \cos \theta d\theta = \frac{l \sin \theta_c}{\theta_c} \quad (24)$$

Where $\theta_c = \cos^{-1}(l_c/l)$ is the critical fiber angle. Only when the fiber angles are smaller than this angle, can these fibers become bridging fibers.

According to Equation 20, the probability for the three dimensional distributed fibers to become bridging fibers is

$$P_b = \begin{cases} 1 - \frac{l_c \theta_c}{l \sin \theta_c} & (\theta < \theta_c) \\ 0 & (\theta > \theta_c) \end{cases} \quad (25)$$

In the fractured surface the total number of bridging fibers is

$$N_b = N_a \times P_b = \frac{\varphi_f}{2\pi r_f^2} \left(1 - \frac{l_c \theta_c}{l \sin \theta_c} \right) \quad (26)$$

The unbridged number of fibers is

$$N_{ub} = N_a - N_b = \frac{\varphi_f l_c \theta_c}{2\pi r_f^2 l \sin \theta_c} \quad (27)$$

The maximum pull-out length for unbridged fiber is $l_c/2$, then the average projecting length of three dimensionally distributed fibers in the tension direction is $l_c/4$. The fiber length contribution function can be written as

$$f(\sigma_{bf}, \sigma_{ubf}) = \sigma_f \pi r_f^2 N_b + 2\pi r_f \frac{l_c}{4} \tau_s N_{ub} \quad (28)$$

Substituting Equations 1, 26 and 27 into Equation 28 gives

$$f(\sigma_{bf}, \sigma_{ubf}) = \frac{1}{2} \left(1 - \frac{l_c \theta_c}{2l \sin \theta_c} \right) \sigma_f \varphi_f \quad (l/l_c > 1), \quad \theta_c = \cos^{-1}(l_c/l) \quad (29)$$

Only the length variation is considered when a fiber in space is projected onto the tension direction. In fact, the tensile stress in the fiber will also change when making projections in the tension direction. This is considered using the factor c in Equation 15. Considering a fiber having an angle θ with the tension direction, the relation between σ_0 and σ_θ is

$$\sigma_\theta = \sigma_o \cos^2 \theta \quad (30)$$

The force in the tension direction for this fiber is

$$F = A_f \sigma_o \cos^3 \theta \quad (31)$$

Where $A_f = \pi r_f^2$ is the cross sectional area of the fiber.

To keep the agreement between the geometrical projection and the stress projection, letting the modification factor be

$$c = \frac{A_{fp}}{A_f} \cos^2 \theta \quad (32)$$

where $A_{fp} = 2\pi r_f^2$ is the projected cross sectional area in the tension direction.

Using θ_a in Equation 22 as the average angle of fibers, then $c = 0.5$.

Substitute Equations 29 and c into Equation 15, the ultimate tensile strength of the fiber reinforced concrete is obtained as follow

$$\sigma_0 = \frac{1}{4} \left(1 - \frac{l_c \theta_c}{2l \sin \theta_c} \right) \sigma_f \varphi_f \quad (l/l_c > 1, \quad \theta_c = \cos^{-1}(l_c/l)) \quad (33)$$

Equation 33 is for fiber length greater than the critical fiber length. The average projecting length of fibers in the aligned direction is $l/2$, then the average pullout length of fibers is $l/4$. Thus the fiber strength contribution function is

$$f(\sigma_{bf}, \sigma_{ubf}) = 2\pi r_f \frac{1}{4} \tau_s N_a \quad (34)$$

Substitute Equations 1, 19, c and 34 into Equation 15, the ultimate tensile strength with fiber length smaller than the critical zone width is

$$\sigma_0 = \frac{l}{8l} \sigma_f \varphi_f \quad (l/l_c < 1) \quad (35)$$

For fiber length longer than the critical the ultimate tensile strength of fiber reinforced concrete can be estimated by Equation 33 and for fiber length shorter than the critical fiber length by Equation 35. If the fiber length varies over a certain range, the axial tensile strength of fiber reinforced concrete can be estimated based on Equations 33 and 35

$$\sigma_0 = \int_{l_{\min}}^{l_c} \frac{l}{8l_c} \sigma_f \varphi_f f(l) dl + \int_{l_c}^{l_{\max}} \frac{1}{4} \left(1 - \frac{l_c \theta_c}{2l \sin \theta_c} \right) \sigma_f \varphi_f f(l) dl \quad (36)$$

Where $f(l)$ is the fiber length distribution density; l_{\min} is the minimum fiber length; l_{\max} is the maximum fiber length.

The length distribution density can be assumed to be unit and Equation (36) integrated to give

$$\sigma_0 = \frac{\sigma_f \varphi_f}{8l_c} \left[\frac{l_c^2}{2} - \frac{l_{\min}^2}{2} \right] + \frac{\sigma_f \varphi_f}{4} [l_{\max} - l_c] - \frac{l_c \theta_c \sigma_f \varphi_f}{2 \sin \theta_c} [\ln l_{\max} - \ln l_c] \quad (37)$$

Equation 36 or 37 is the overall equation for predicting the ultimate tensile strength of fiber reinforced concrete.

The models that have been developed above are for circular cross sectional area fibers. The development of models for square cross sectional area fibers is an extremely tedious process. Since the fibers used in the experiments were of a square cross sectional areas, equivalent circular fibers were obtained. The finite element model below along with a short numerical analysis was used to obtain the geometry and

properties of the equivalent circular fiber. Finite element modeling was done based on various criteria such as Von Mises stress, maximum stress, maximum strain and stress intensity to see which one gave the closest results to the square fiber concrete model. The maximum stress intensity was chosen as the criteria to be used.

The dimensions of the square fibers used for analysis were 5 mm x 5 mm x 50.8 mm. In obtaining the equivalent circular geometry, it was assumed that the length of the circular fiber was equal to the length of the square fiber. The volume of the square fiber was equated to the volume of the circular fiber, $50.8 \pi r^2$. The radius of the circular fiber was obtained as 2.82 mm.

CHAPTER 5: FINITE ELEMENT ANALYSIS OF EQUIVALENT FIBER

5.1 Modeling

Finite element analysis, determines the overall behavior of a structure by dividing it into a number of simple elements, each of which has well-defined mechanical and physical properties. The simulations were performed with ANSYS 8.1 finite element software. The fibers used in conducting the experiments were of a square cross sectional area. This geometry had to be converted to an equivalent circular geometry for analysis. The rubberized concrete was treated as a two-phase composite with waste tires dispersed in concrete matrix. The element chosen to simulate concrete was SOLID65 while SOLID185 was used to simulated rubber. SOLID65 has the ability to include non-linear material model such as the Drucker-Prager model that was used to model the plastic behavior of concrete. A simulation was run in ANSYS first for an element of the square model. A cylindrical model was created in ANSYS with all the same properties as the square model. The Young's modulus was varied until similar results were obtained as the square model. When this value was obtained, it was inputted into the equations derived in the analytical model to calculate the critical fiber length and the ultimate tensile strength. The values obtained were compared to the values obtained from the experimental analysis.

Since concrete deforms plastically, both linear elastic properties and plastic properties were defined. In the linear region, the concrete was treated as linear isotropic so only Young's modulus and Poisson's ratio were used. The compressive strength of the concrete was used as 40MPa, initial Young's modulus was 30GPa, and Poisson's ratio was 0.2. Once the concrete yields, the three parameter Drucker-Prager plasticity model takes over the behavior of the concrete. The three parameters necessary to define the Drucker-Prager model are the cohesion, angle of internal friction and the

dilatancy angle. The cohesion was used as 12 MPa, the angle of internal friction as 32° and the dilatancy angle as 8° .

5.2 Meshing

Mesh generation for the three-dimensional models was performed using ANSYS preprocessor. Adequate mesh refinement is always an issue when conducting a finite element analyses. The idea is to have enough refinement to capture all strain gradients of interest, but to avoid excess refinement, which can lead to unnecessarily long run-times.

For a coarse mesh (fewer elements) ANSYS has less number of equations to solve simultaneously so the processing time will be shorter than if a fine mesh was used (more elements). The coarser mesh may not accurately capture the behavior of the model though. A very finely meshed model will usually capture the necessary detail in the system but at the expense of processing time. Therefore, it is necessary to find a compromise when meshing the model. To do this the model was run initially with a coarse mesh. It was run again with a finer mesh a few more times and the results compared each time with the previous result to compare the deviations.

5.3 Simulation

All the degrees of freedoms at one end were constrained to represent one end held fixed and a compressive load was applied to the other end as shown in Figure 8. A large static displacement linear analysis was performed. This was to ensure that any effects of large deflections were included in the results. The Automatic Time Stepping feature was turned on; this enables ANSYS to determine appropriate sizes to break the load steps into. Decreasing the step size usually ensures better accuracy, however this increases the processing time. The Automatic Time Step feature was used to determine an appropriate balance. The number of substeps used for the simulation was 100. This

sets the initial substep to 1/100th of the total load. The maximum number of iterations was chosen as 1000.

To ensure convergence to the correct solution by the finer sub-division of the mesh, the assumed displacement function must satisfy the convergence criteria given below:

- Displacements must be continuous over the element boundaries.
- Rigid body movements should be possible without straining.
- A state of constant strain should be reproducible.

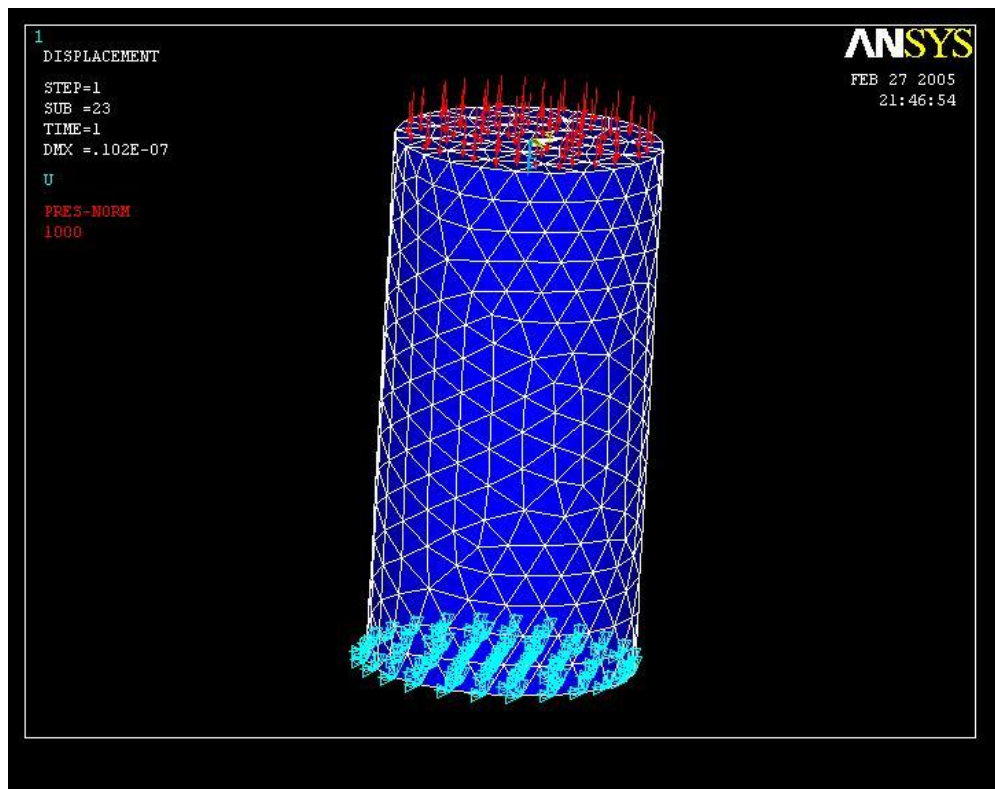


Figure 8: Constraints and load applied to model.

5.4 Solution

A pure compression failure of concrete is unlikely. In a compression test, the specimen is subjected to a uniaxial compressive load. Secondary tensile strains induced by Poisson's effect occur perpendicular to the load. Because concrete is much weaker in tension than compression, these actually cause cracking and the eventual failure.

Therefore, in this study, the crushing capability was turned off and cracking of the concrete controlled the failure of the finite element models.

Cracking and crushing are determined by a failure surface. Once the failure surface was surpassed, concrete cracks if any principal stress was tensile. The failure surface for compressive stresses was based on Willam-Warnke failure criterion [Willam, 1975]. Tensile failure consists of a maximum tensile stress criterion, a tension cutoff. Unless plastic deformation is taken into account, the material behavior is linear elastic until failure. When the failure surface was reached stresses in that direction had a sudden drop to zero, there was no strain softening neither in compression nor in tension. To determine where cracks were formed, a non-hidden, vector type of display was used. ANSYS uses small circles to represent where concrete has cracked. Two shear transfer coefficients, one for open cracks and another for closed ones, were used to consider the retention of shear stiffness in cracked concrete.

SOLID65 has eight integration points at which cracking checks were performed. It behaved in a linear elastic manner until the specified tensile strength was exceeded. Cracking of an element was initiated once one of the element principal stresses, at an element integration point, exceeded the tensile strength of the concrete. Cracked regions, as opposed to discrete cracks, were then formed perpendicular to the relevant principal stress direction with stresses being redistributed locally. Subsequent to the formation of an initial crack, stresses tangential to the crack face may cause a second, or third, crack to develop at an integration point.

When a compressive load is applied to concrete, many micro-cracks develop in the structure. These cracks are responsible for the failure of concrete. ANSYS was able to show the first, second and third micro-cracks that were formed on the application of load. Figure 9 shows the first micro-cracks for the simulation. The 'first crack' is the stage at which microscopic parts of the paste or paste and aggregate separate.



Figure 9: First cracks formed in concrete surrounding fiber on application of load.

CHAPTER 6: RESULTS AND DISCUSSION

6.1 Compressive and Tensile Strength of Concrete

The results of the tests for strength performed on the samples in the experiments are shown below.

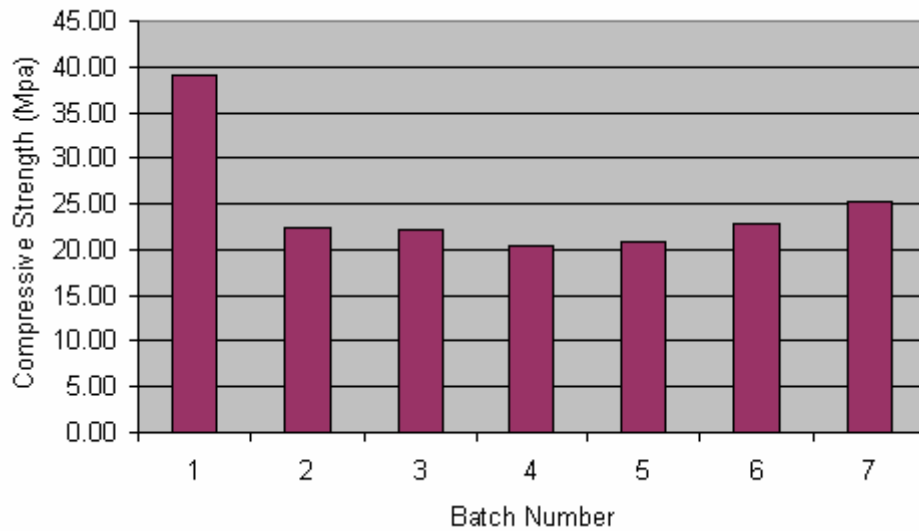


Figure 10. Variation of the compressive strength of concrete.

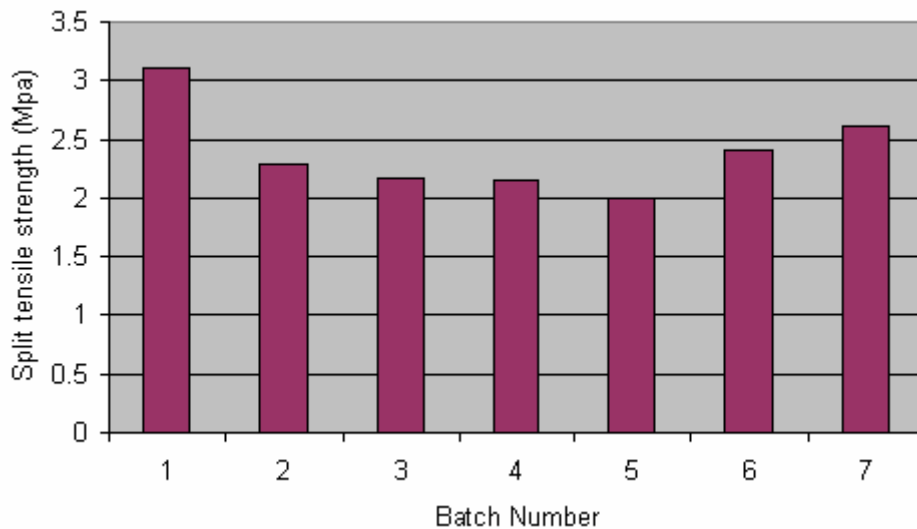


Figure 11: Variation of split tensile strength of concrete.

It can be seen from Figure 10, that there was a significant and almost consistent decrease in the compressive strength of the rubberized concrete batches. Of all the batches tested the control batch had the highest compressive strength. There was

approximately 43% decrease in the compressive strength with the addition of the waste tire chips. Batch 7, which was composed of the waste mixed tire in a fibrous form, had the highest compressive strength of all the modified samples.

Figure 11 shows that the control samples had the highest split tensile strength. Batches 3-5, which consisted of waste tires without steel wire, had the lowest split tensile strengths. Batch 7 had the highest split tensile strength of all the rubberized concrete samples. This batch consisted of the waste tires with the highest modulus of elasticity and had the most steel wires included.

This implies that it is advantageous to include waste tires with wires and high modulus of elasticity into the concrete. This is further supported by the fact that batch 6 which contained car tires with wires had a higher split tensile strength than batches 3-5 which contained car tires without wires. The introduction of waste tires into concrete reduced its split tensile strength. The reduction of strength can however be minimized by including tires with higher elastic modulus such as truck tires and specifically tires that contain wires.

The strength was reduced in waste tire modified concrete for several reasons including:

- The inclusion of the waste tires acted like voids in the matrix. This is because of the weak bond between the waste tire and concrete matrix. With the increase in void content of the concrete, there will be a corresponding decrease in strength. The weakness of the bond between the waste tires and cement matrix can be seen by how easy it is to remove the fibers from the crushed sample by simply using ones fingers.
- Waste tires act as weak inclusions in the hardened cement mass and as a result produced high internal stress that are perpendicular to the direction of applied load.

- Portland cement concrete strength is dependent greatly on the coarse aggregate, density, size, and hardness. Since the aggregates are partially replaced by rubber, the reduction in strength is only natural.
- The failure of the sample is also because of the waste tire being more elastically deformable than the matrix. When the samples were loaded the cracks form first at the softest areas. The site of the inclusion of rubber is where these sites appear.

The tensile strength of concrete is much lower than the compressive strength, largely because of the ease with which cracks can propagate under tensile loads. Although tensile strength is usually not considered directly in design, its value is still needed because cracking in concrete tends to be of tensile behavior. Concrete can be considered as a brittle material, and the tensile strength of a brittle material is due to the rapid propagation of a single flaw or microcrack.

6.2 Modulus of Elasticity

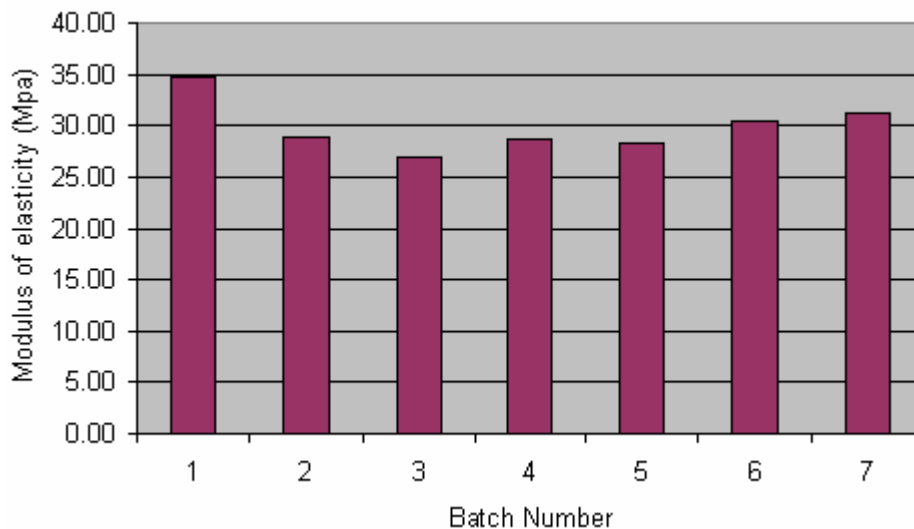


Figure 12: Variation of modulus of elasticity of concrete.

Figure 12 shows that the control sample possessed the highest modulus of elasticity. The general deviation in values for the rubberized samples was rather small. The 2-inch

truck and car tire with steel had the highest value of all the rubberized samples. The volume and modulus of the aggregate are the factors that are mainly responsible for the modulus of elasticity of concrete. Therefore, small additions of tire fiber would not be able to significantly change the modulus of the composite.

6.3 Workability of Concrete

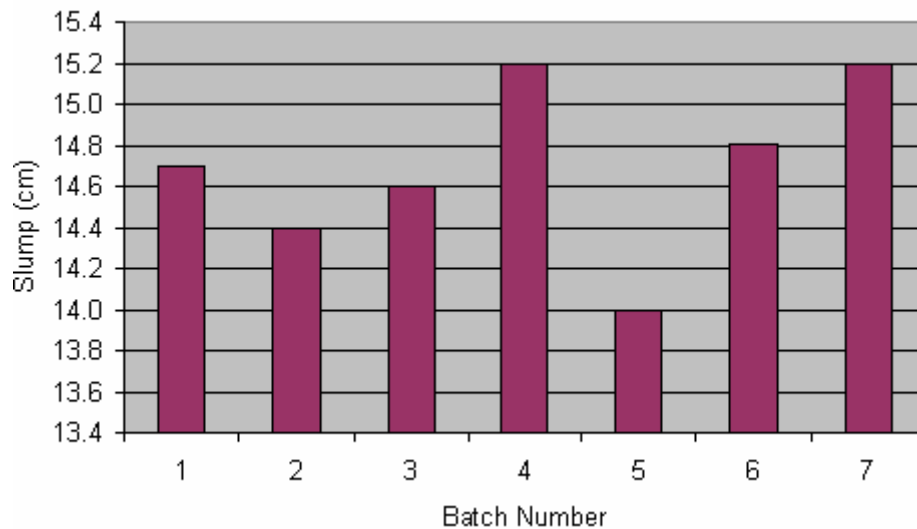


Figure 13: Variation of slump of concrete.

One of the concerns when adding waste tires to the concrete was whether the workability of the concrete would be negatively affected. Workability refers to the ability of the concrete to be easily molded.

From Figure 13 it was seen that there was a variation of approximately +/- 0.7 between the slump of the control samples and the rubberized concrete. Also, Figure 14 shows that the variation of air content in the different batches was not significant. These results imply that the workability of the concrete was not adversely affected by the addition of waste tires.

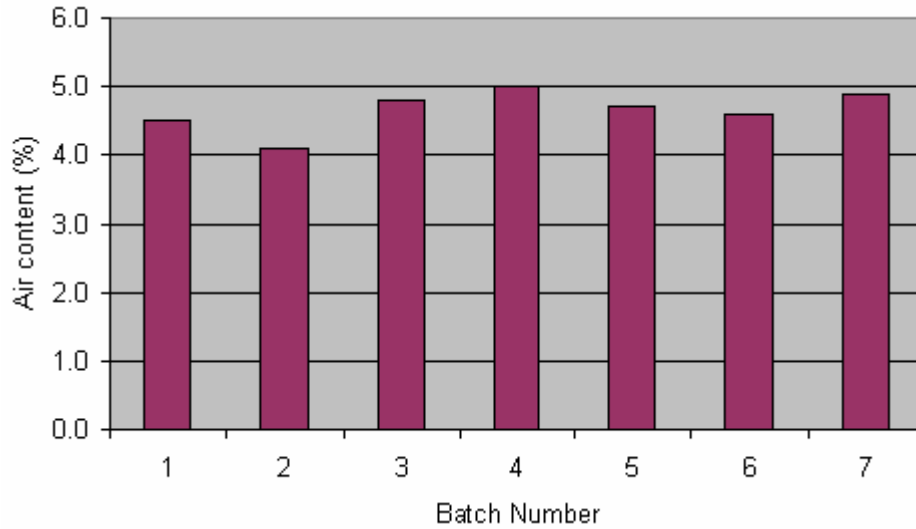


Figure 14: Results of air content for concrete.

6.4 Effect of Waste Tire on Toughness of Concrete

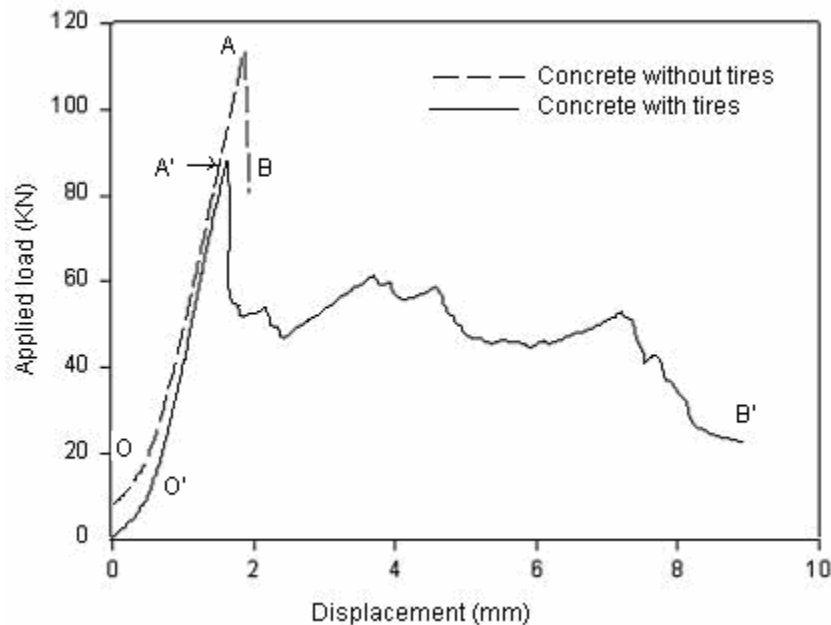


Figure 15: Load displacement results for split tensile testing of rubberized and plain concrete.

Figure 15 shows the applied load - displacement curves for split tensile testing of a control sample and a rubberized sample from batch 7. The concrete without waste tire failed a lot sooner than the rubberized concrete. Toughness, which is the energy

absorbed by the sample is measured by the area under the curve. It can be seen that the area beneath the curve for the concrete without rubber is very small compared to the area beneath the curve for the concrete with rubber. This implies that concrete with rubber is much tougher than concrete without rubber.

Toughness describes how a material will react under sudden load. With its increased toughness, rubberized concrete will be able to resist crack propagation, catastrophic failures and absorb dynamic loads more than the control.

It was observed that the samples tend to fail more gradually with the addition of waste tires. Waste tire modified samples were able to undergo a higher deformation than the control mix. The ability of the sample to deform elastically has thus increased.

The high elastic energy capacity of normal concrete was reduced after adding rubber while the plastic energy capacities began to increase. As a result of their high plastic energy capacities these concrete showed high strains especially under impact effects.

From Figure 15, it was seen that after maximum stress (cracks growing inside concrete matrix), the graph continues when the concrete contains fibers. In concrete without fibers, the first crack propagates immediately, causing instant failure. In waste tire modified concrete the rubber maintained the sides of the crack together, allowing the material to retain a part of the load at large displacement.

The portion OA and O'A' are common to most type of composites. They represent the stage in which the matrix carries the stress and the role of the fibers is relatively unimportant. The portions AB and A'B' represent the stage in which stress is progressively transferred from the matrix to the fibers. The former had a sudden and short decline because the matrix had no fibers to carry the stress after the control sample reach its ultimate stress.

A'B' is typical of some short, randomly oriented fiber. The shape of the curve A'B' is controlled by many factors including the sliding friction bond strength for fibers at random angles, the aspect ratio of the fibers, the fiber volume fraction and the composition of the matrix. A'B' is more desirable than AB since the former implies increased toughness.

6.5 Ductility of Concrete

Concrete without waste tire, shows brittle behavior as can be clearly seen from Figure 16. In rubberized concrete, the post-cracking ductility form a major part of the load carrying system since the load is now being carried by the fibers and not the matrix. The post cracking ductility imparted by the fibers is very important. It too can be determined by calculating the area under the load-deflection curve. Concrete reinforced with waste tire fibers have high impact and shatter resistance due to the large amount of energy absorbed in debonding, stretching, and pulling out the fibers which occur after the matrix is cracked.

Cracks formed will propagate in the matrix until they get to the waste tire aggregate. The aggregates act like springs since they are able to withstand large tensile deformations. They therefore reduce the widening of the cracks and minimize disintegration of the concrete matrix. More cracks will continue to form and those that are already present will continue to widen with the continued application of compressive load. The sample is thus absorbing a lot of plastic energy and resisting large deformation without full disintegration. This continues for a period of time. The concrete samples were able to withstand loads even when they had significant cracks. Failure only occurs after the stresses overcame the bond between the cement matrix and the rubber aggregate.

The ductility of the concrete depends on the strength of the bond between the fibers and matrix and the volume of the fibers. These variables, together with the length efficiency factors and fiber orientation will result in a range of stress-strain curves or ductility. Other factors that affect the post cracking behavior include the number of fibers and the effective fiber orientation.

Table 3: Efficiency factors, η_1 , for a given fiber orientation relative to the direction of stress.

Fiber Orientation	η_1 [Cox, 1952]	η_1 [Krenchel, 1964]
1-D aligned	1	1
2-D random	1/3	3/8
3-D random	1/6	1/5

Aligned fibers will have a much greater effect on the material properties of the sample under direct stress in the uncracked state than non-aligned fibers. For short random fibers, such as those used in the waste tire reinforced concrete, which are generally shorter than the critical length for fiber breakage, pull out mostly occurs across a crack.

The bond stress depends on a variety of factors such as water/cement ratio, curing conditions, fiber surface characteristics, fiber geometry, and age. For low fiber volume the composite may be expected to crack at about the same stress as the matrix. However, the inclusion of the fibers prevents the rapid disintegration of the concrete. After the matrix is cracked, there is a linear transfer of stress from the fibers bridging the crack back into the matrix.

6.6 Waste Tire Chips versus Waste Tire Fibers

On comparing the results obtained from the experiments for the waste tire chips versus the waste tire fiber modified concrete it was found that the samples with waste tire fibers were stiffer and stronger than the samples with waste tire chips. Waste tire

fibers were thus able to improve the qualities of the concrete more than waste tire chips. The toughness for both waste tire chip and waste tire fiber modified concrete was greater than the toughness of the control; however waste tire fiber modified samples were tougher than waste tire chip modified samples. It was also found that the strength of both types was lower than the control samples.

There was a general reduction in compressive strength for rubberized concrete. The waste tire fiber modified concrete however gave better results than the waste tire chip modified concrete. This is because more stress concentrations are formed in the samples with the chips than in the fibrous samples. In Figure 14, it was seen that the air content of all the fibrous samples was greater than for batch with chips.

6.7 Analytical and Finite Element Results

The ANSYS model was used to simulate the compression of the unmodified and rubberized concrete. For the latter it was assumed that the waste tires used had inclusions of steel fibers and were from truck tires, hence they had high stiffness. Simulations were performed on the square model then on the circular model with all the same properties except for the Young's modulus. Young's modulus was varied for the circular model until results similar to the square model were obtained for parameters such as the stress intensity and Von Mises stress.

The value of Young's modulus obtained for the circular fiber was 2 GPa. When this value was substituted into Equation (11), the critical fiber length was obtained as 7 inch. Seven inches is the theoretical value for the critical length, however this is not feasible to be used in the experiments for the following reasons:

- The fibers would become entangled with each other. If during mixing the fibers could be prevented from being entangled, this would be the best length to use. At the moment there is no technology to prevent this from occurring so we had to use

the next best length that would give enough strength yet would significantly reduce the entanglement, thus the 1, 2 and 3 inch lengths were used. If the fibers were allowed to bunch they would not be able to impart strength uniformly throughout the composite, thus the benefits of using fiber reinforcement in concrete would not be fully displayed.

- Also because of the size of the formwork used to make the samples was just 6 inch in diameter and 12 inch in height, there was no way that 7-inch long fibers could possibly be distributed evenly in the sample.

The 2-inch fibers performed best as their properties were able to be distributed evenly throughout the composite.

When the critical length of 7 inch and the actual value of 2 inch used in the experiment were substituted into the Equation 39 the ultimate tensile strength obtained was 2.49 MPa. This was very close to the actual value obtained from the experiment of 2.62 MPa.

Table 4. Values used in calculations.

Properties	Values
Radius (r)	0.00159 m
Modulus of elasticity of matrix (E_m)	30×10^9 Pa
Modulus of elasticity of fiber (E_f)	2×10^9 Pa
Shear modulus of matrix (G_m)	12.5×10^9 Pa
Volume fraction of effective space (f_e)	0.9097
Volume fraction of fibers in concrete (f_{fc})	0.15
Volume fraction of matrix (v_m)	0.2
Critical length (L_c)	0.1778 m
Ultimate strength of fiber (σ_f)	29.58×10^6 Pa
Frictional shear strength at fiber-matrix interface	55.08×10^6 Pa

Due to the difficulty in cutting the waste tires with the equipment available, it was not possible to cut the tires as thin as was desired. The dimensions of the cross

sectional area of the fibers used was 5mm by 5mm. The aspect ratio of the fibers, which is the length of the fibers divided by its diameter, ranged from 5 to 15. An aspect ratio of approximately 30 was desired to get the maximum benefits from the fibers. The aspect ratio determines the efficiency of the load transfer from the matrix to the fiber. The larger the aspect ratio, the more efficient is the load transfer.

In addition, for fibers with the same length but different cross sectional areas, the fibers with the lower aspect ratio will occupy a greater volume. It was mentioned previously that voids cause a decrease in strength, thus the fibers with the lower aspect ratios would act as bigger voids, hence decreasing the strength more than higher aspect ratio fibers.

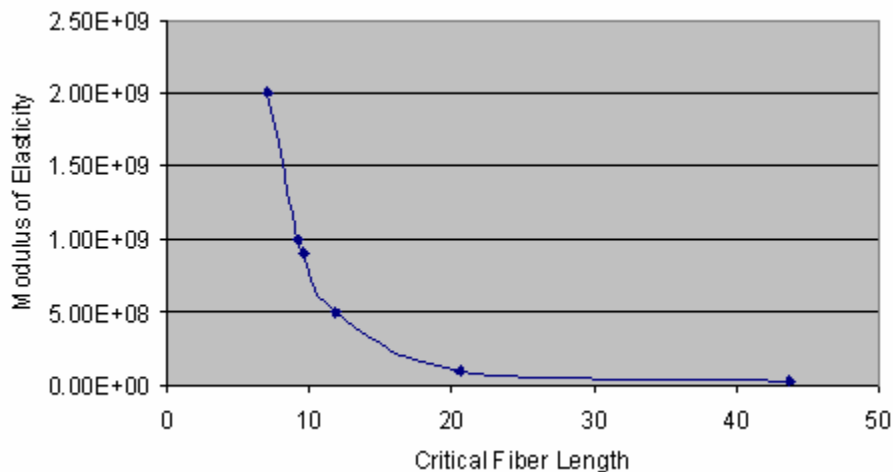


Figure 16: Variation of critical fiber length with modulus of elasticity

A parametric study was done to see how the modulus of elasticity or stiffness would affect the critical fiber length of the waste tires. It can be seen from Figure 16 that the stiffer the fiber the lower the critical fiber length will be. This supports the experimental results that stiffer fibers such as truck tires with steel wires were more desirable as reinforcements.

From Figures 16 it can be seen that the modulus of elasticity played a very important role in waste tire modified concrete. It affected both the critical fiber length and the ultimate tensile strength.

6.8 Uses of Waste Tire Modified Concrete

Waste tire modified concrete can be used in industrial floorings such as factory and warehouse floors where the increased impact resistance and post-cracking ductility will be beneficial. The properties which are important from the point of view of pavement performance are increased flexural strength, improved post-cracking ductility, increased resistance to impact and repeated loading and improved spalling resistance.

Waste tire concrete can be use in applications where energy and impact attenuation is required due to its high flexibility. Unlike the control concrete which disintegrated when the peak load was reached, the rubberized concrete underwent a considerable deformation without disintegration. In fact, the control concrete sample broke into two halves after unloading, while the rubberized concrete sample kept its integrity and the crack opening width was reduced, and sometimes even closed. This suggests that rubberized concrete offer a great potential for it to be used in sound/crash barriers, retaining structures, and pavement structures if its strength is appropriate

CHAPTER 7: CONCLUSION

Concrete mixes were prepared both with and without waste tire rubber. For those with waste tires, there was one batch made with waste tires in the form of chips while the others were made with waste tires as fibers with different aspect ratios. Numerical analysis, finite element analysis and experimentations were conducted. Several conclusions were reached:

- The toughness of waste tire modified concrete was much greater than unmodified concrete. It was thus able to absorb more energy when loaded than the control sample.
- Owing to the fibers bridging over the cracks, the crack opening width can be controlled. In addition the three dimensional distribution of fibers in concrete provides the reinforced concrete with improved performance in all directions.
- Waste tire modified concrete failed in a ductile manner rather than a brittle manner.
- The sample with waste tire as fibers performed better than those with chips thus, waste tires should be used as fibers instead of chips.
- It is not very beneficial to include fibers in cement matrices to increase the first tensile strength. The effect of the fibers on the concrete is not fully realized until cracking has occurred, as this is when the load carrying ability of the fiber comes into effect.
- The critical fiber length as obtained from the numerical analysis was 7 inch. It was not however feasible to use this length of fiber due to fiber entanglement that would result and because of the size of the formwork used to make the samples. It is recommended not to use fiber lengths exceeding 3 inches since fibers will bunch

together. The workability of concrete was not negatively affected by the inclusion of waste tires 3 inches and less.

- The finite element model clearly showed the development of microcracks in the concrete. The model can be used to try and keep the formation of cracks to a minimum, thus increasing the strength at which concrete fails.
- Waste tire modified concrete had lower compressive and tensile strength than the control mix. It was however shown that it was advantageous to use stiffer fibers as they had higher strengths.
- Waste tires can be included to increase the ductility in compressive failure. One of the major benefits of waste tire fibers is the holding together of a cracked area after minor impacts.
- The present model used in the analytical modeling is valuable and useable to predict the ultimate tensile strength of fiber reinforced concrete.
- From the results obtained from this study it was determined also that the geometry of the fibers also had an influence on the strength of the concrete. The aspect ratio of the waste tire fibers needs to be increased.
- In fiber reinforced concrete, the major effect of the fibers has been noted in the post-cracking case, where the fibers bridge across the cracked matrix.

REFERENCES

Agarwal, B.D., Broutman, L.J., "Analysis and Performance of Fiber Composites", John Wiley & Sons, New York, 1980

Allen, H.G., "Glass-fiber reinforced cement, strength and stiffness," CIRIA Report 55, September, 1975.

American Society for Testing and Materials, Standard Method of Test for Splitting Tensile Strength of Cylindrical Concrete Specimens (ASTM C496-86), Philadelphia, 1986.

ANSYS User's Manual 9.0: Ansys structural analysis guide.

Barbosa, Antonio F., Ribeiro, Gabriel O., "Analysis of reinforced concrete structures using ANSYS nonlinear concrete model," Computational Mechanics, New Trends and Applications, Barcelona, Spain 1998.

Cox, H. L., "The Elasticity and Strength of Paper and other Fibrous Materials," British Journal of Applied Physics, Vol. 3, 1952, pp.72-79.

Edginton, J., Hannant, D.J., and Williams, R.I.T., "Steel-fiber-reinforced concrete," Building Research Establishment Current Paper CP 69/74, July 1974.

Eldin, N. N., and Senouci, A. B., "Rubber-tire particles as concrete aggregate." Journal of Material in Civil Engineering, ASCE, 5(4), 1993, 478–496.

Elvery, R. H., and Samarai, M.A., "Reduction of shrinkage cracking in reinforced concrete due to the inclusion of steel fibers," Fiber-reinforced Cement and Concrete, RILEM Symposium, 1975, pp. 149-159.

Epps, J. A., "Uses of recycled rubber tires in highways" Synthesis of highway practice 198, Transportation Research Board, National, 1994.

Fanning, P., "Nonlinear Models of Reinforced and Post-tensioned Concrete Beams," Electronic Journal of Structural Engineering, 2 (2001), pp. 111-119

Hannant, D. J., Fiber Cements and Fiber Concretes, John Wiley and Sons, New York, 1978.

Hernandez-Oliveres, F. and Barluenga, G., "Fire performance of recycled rubber-filled high-strength concrete" Cement and Concrete Research, Vol 34, No. 1-3, (2003) pp 109-117.

Hoff, G. C., "The use of fiber reinforced concrete in hydraulic structures and marine environments," Fiber reinforced Cement and Concrete, RILEM Symposium, 1975, pp. 395-407, Construction Press Ltd.

http://www.cement.org/basics/concretebasics_faqs.asp, November 25, 2003.

<http://www.moxie-intl.com/glossary.htm>, November, 3, 2004.
<http://www.nrmca.org/aboutconcrete/cips/CIP%2022p.pdf>, September 20, 2003.

<http://www.p2pays.org/ref/11/10504/html/usa/overview.htm>, October, 10, 2004.
<http://www.rma.org> , August 15, 2004.

Johnston, C.D., "Steel-fiber-reinforced concrete pavement-second interim performance report," Fiber-reinforced Cement and Concrete, RILEM Symposium, 1975, pp. 409-418.

Kelly, A., Aveston, A., and Cooper, G.A., Single and Multiple Fracture, The Properties of Fiber Composites, Proc. Conf. National Physical Laboratories, IPC, Science and Technology Press, UK, 1971.

Khatib, Z., K., and Bayomy, F. M., "Rubberized Portland Cement Concrete," Journal of Materials in Civil Engineering, Vol. 11, No. 3, (1999), pp. 206-213.

Krenchel, H., Fiber Reinforcement, Akademisk Forlag, Copenhagen, 1964.

Kullaa, J, "Constitutive modeling of fiber-reinforced concrete under uniaxial tensile loading," Composites, Vol. 25, No. 10, 1994.

Lee, B. I, Burnett, L., Miller, T., Postage, B., Cuneo, J., "Tire rubber/cement matrix composites," Journal of Material Science Letter, Vol. 12, No. 13 (1993) pp. 967-968.

Mehta, P. K., and Monteiro, P. J. M., Concrete Structure, Properties, and Materials, 2nd Ed., Prentice-Hall, Englewood Cliffs, N.J., 1993

Neville, A. M., "Properties of Concrete," 4th Edition, New York, J. Wiley, 1996

Proceedings of the Symposium on Fibrous Concrete, Fibrous concrete, The Concrete Society, The Construction Press Ltd, Lancaster, England, 1980.

Raghavan, D., Huynh, H., Ferraris, C.F., "Workability, mechanical properties and chemical stability of a recycled tire rubber-filled cementitious composite," Journal of Material Science, Vol. 33 (1998) pp.1745-1752.

Segre N., Joekes N., "Use of tire rubber particles as addition to cement paste," Cement and Concrete Research, Vol. 30 (2000) 1421-1425.

Smith, D. M., and Chughtai, A. R., "The surface structure and reactivity of black carbon", Colloid Surface A, (1995), pp. 47-77.

Snyder, J. M., and Lankard, D. R., "Factors Affecting the Flexural Strength of Steel Fibrous Concrete," Journal American Concrete Institute, Title No. 69-9, (1972), pp.96-100.

Topcu, I. B., "The properties of rubberized concretes," Cement and Concrete Research, Vol. 25, No. 2, (1995), pp. 304-310.

U.S. Environmental Protection Agency et al, Scrap Tire Technology and Markets Noyes Data Corporation, NJ 1993.

Wang, Y., "Mechanics of fiber reinforced concrete" Master of Science Thesis (Department of Mechanical Engineering, Massachusetts Institute of Technology, 1985 pp.175)

Willam, K. J., and Warnke, E. D., "Constitutive model for the Triaxial Behavior of Concrete," Proceedings, International Association for Bridge and Structural Engineering, Vol. 19, ISMES, Bergamo, Italy, (1975), pp. 174

Zaher, K. K., Bayomy, F. M., "Rubberized Portland Cement Concrete" Journal of Materials in Civil Engineering, Vol. 11, No. 3, 1999, pp. 206-213.

VITA

Gregory Garrick was born in St. Catherine, Jamaica. He obtained his Bachelor of Science in Mechanical Engineering degree from Louisiana State University in December 2001. He joined the master's program in mechanical engineering in the summer of 2002. He expects to graduate in May 2005.